BIOCHEMISTRY
including biophysical chemistry & molecular biology

ARTICLE

pubs.acs.org/biochemistry

# Mechanism of Amyloid β-Protein Aggregation Mediated by GM1 Ganglioside Clusters

Keisuke Ikeda,† Takahiro Yamaguchi, Saori Fukunaga, Masaru Hoshino, and Katsumi Matsuzaki*

Graduate School of Pharmaceutical Sciences, Kyoto University, 46-29 Yoshida-Shimoadachi-cho, Sakyo-ku, Kyoto 606-8501, Japan

Supporting Information

**ABSTRACT:** It is widely accepted that the conversion of the soluble, nontoxic amyloid β-protein (Aβ) monomer to aggregated toxic Aβ rich in β-sheet structures is central to the development of Alzheimer's disease. However, the mechanism of the abnormal aggregation of Aβ in vivo is not well understood. We have proposed that ganglioside clusters in lipid rafts mediate the formation of amyloid fibrils by Aβ, the toxicity and physicochemical properties of which are different from those of amyloids formed in solution. In this paper, the mechanism by which Aβ-(1−40) fibrillizes in raftlike lipid bilayers composed of monosialoganglioside GM1, cholesterol, and sphingomyelin was investigated in detail on the basis of singular-value decomposition of circular dichroism data and analysis of fibrillization kinetics. At lower protein densities in the membrane (Aβ:GM1 ratio of less than ∼0.013), only the helical species exists. At intermediate protein densities (Aβ:GM1 ratio between ∼0.013 and ∼0.044), the helical species and aggregated β-sheets (∼15-mer) coexist. However, the β-structure is stable and does not form larger aggregates. At Aβ:GM1 ratios above ∼0.044, the β-structure is converted to a second, seed-prone β-structure. The seed recruits monomers from the aqueous phase to form amyloid fibrils. These results will shed light on a molecular mechanism for the pathogenesis of the disease.

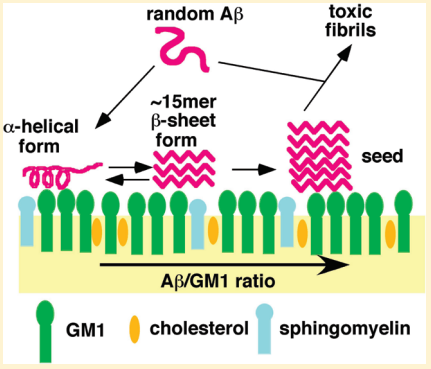


Amyloids are involved in the pathogenesis of more than 20 diseases, including severe neurodegenerative disorders such as Alzheimer's disease (AD), Parkinson's disease, Huntington's disease, and Creutzfeldt-Jakob disease. The kinetics of protein fibrillation in solution have been investigated extensively.[1−6] Today, the most convincing model for the kinetics of amyloid fibril formation is the nucleation-dependent polymerization model, in which the fibrillation process is separated into two steps. A seed for aggregation is formed by self-association and structural changes of monomeric proteins, followed by the binding of monomers to the seed or a preformed fibril end. The bound protein acts as a new binding site for polymerization. A lag phase is observed in the time course of aggregation, because the seed's formation is the rate-limiting step. Compared to aggregation kinetics in solution, little attention has been paid to the kinetics of protein aggregation mediated by membranes despite its biological significance. Accumulating evidence suggests that lipid−protein interactions play a crucial role in the aggregation of various amyloidogenic proteins.[7,8] The formation of fibrils on membranes is more complicated because both membrane-bound and unbound molecular species can participate in the aggregation.

The aggregation of the 39−42-residue amyloid β-protein (Aβ) into oligomers and fibrils is a critical step in the etiology of AD. AD is a progressive neurodegenerative disorder, hallmarks of which are the deposition of amyloid fibrils and the formation of neurofibrillary tangles.[9,10] The mechanism of the abnormal aggregation of Aβ is not well understood. The physiological concentration of Aβ in biological fluids ($<10^{-8}$ M)[11] is much lower than the concentration (∼1 μM) above which Aβ-(1−40) spontaneously forms fibrils.[12] Therefore, there should be mechanisms that facilitate the abnormal aggregation of Aβ under pathological conditions. We have proposed that ganglioside clusters in lipid raft microdomains play a crucial role in the formation of amyloid fibrils by Aβ.[13,14] Aβ interacts with monosialoganglioside GM1 (GM1) in model membranes mimicking lipid rafts under physiological conditions.[15] GM1 is an acidic glycosphingolipid abundant in plasma membranes of neurons and has been thought to be involved in the pathology of AD.[14,16,17] Aβ recognizes and binds to a GM1 cluster, changing its conformation from a random coil to an α-helix-rich structure at lower protein densities on the membrane and to a β-sheet-rich structure at higher protein densities. The fibril-forming process is accelerated in the presence of the β-sheet form of Aβ.[18] However, the details of the α-helix−β-sheet transition and the subsequent fibrillization are yet to be clarified.

In this paper, the structural changes of Aβ-(1−40) on GM1-containing raftlike membranes composed of GM1, cholesterol, and sphingomyelin were investigated in detail by circular dichroism (CD) after correction of spectral contributions from free proteins in solution. A singular-value decomposition (SVD) analysis revealed that the α-helix−β-sheet transition occurred highly

**Received:** May 19, 2011
**Revised:** June 14, 2011
**Published:** June 17, 2011

cooperatively above a threshold intramembrane protein concentration. The β-sheet structure was composed of ∼15 Aβ molecules and did not form fibrils. A seed-prone β-structure was produced only at higher concentrations. Furthermore, a kinetic study indicated that the seed recruited not membrane-bound monomers but free proteins in solution to form amyloid fibrils.

## MATERIALS AND METHODS

**Aβ** Aβ-(1−40) was produced as a ubiquitin extension[19] and purified as described in detail elsewhere.[20] The purity (>95%) and identity of the protein were confirmed by analytical reversed-phase high-performace liquid chromatography (HPLC) and electrospray ionization mass spectroscopy. The protein was dissolved in 0.02% ammonia on ice, and any large aggregates that may act as a seed for aggregation were removed by ultracentrifugation in 500 μL polyallomer tubes at 540000*g* and 4 °C for 3 h. The protein concentration of the supernatant was determined in triplicate with a Micro BCA protein assay (Pierce, Rockford, IL). The supernatant was collected and stored at −80 °C prior to use. Just before the experiment, the stock solution (∼300 μM) was mixed with an equal volume of doubly concentrated buffer [11.5 g/L NaF, 2.3 g/L $Na_2HPO_4$, and 0.4 g/L $KH_2PO_4$ (pH 7.4)], and the final protein concentration was adjusted to the desired value by addition of a buffer [5.75 g/L NaF, 1.15 g/L $Na_2HPO_4$, and 0.2 g/L $KH_2PO_4$ (pH 7.4)] and/or a vesicle suspension. NaF and phosphate were used to reduce UV absorption by buffer components and thus to improve the signal-to-noise ratio.[21] Aβ-(1−40) assumes a monomeric state under these conditions.[22]

**Small Unilamellar Vesicles (SUVs).** GM1 from bovine brain was purchased from Wako (Osaka, Japan). Cholesterol and *N*-acyl-D-sphingosine-1-phosphocholine from bovine brain (SM) were obtained from Sigma (St. Louis, MO). SUVs were prepared as described previously.[15,18] GM1, cholesterol, and SM were dissolved in a 1:1 (v/v) chloroform/methanol mixture, chloroform, and ethanol, respectively. The concentrations of GM1, cholesterol, and SM were determined at least in triplicate by the resorcinol−hydrochloric acid method,[23] the cholesterol oxidase method (free cholesterol E-test kit from Wako), and the phosphorus assay,[24] respectively. GM1, cholesterol, and SM were mixed in a molar ratio of 4:3:3, and the solvent was removed by evaporation in a rotary evaporator. The residual lipid film, after drying under vacuum overnight, was hydrated with a buffer [5.75 g/L NaF, 1.15 g/L $Na_2HPO_4$, and 0.2 g/L $KH_2PO_4$ (pH 7.4)]. The hydrated film was vortex mixed to produce multilamellar vesicles, which were subsequently sonicated under a nitrogen atmosphere for 9 min (3 × 3 min) using a UD-201 probe-type sonicator (Tomy, Tokyo, Japan). Metal debris from the titanium tip of the probe was removed by centrifugation. The concentration of vesicles was determined on the basis of the concentration of GM1 (4 mM).[25] The vesicles have been characterized in terms of size and lamellarity.[26]

**Binding of Aβ.** Aβ (50 μM) was mixed with GM1/cholesterol/SM SUVs in the buffer described above and equilibrated for 5 min at 37 °C. The free Aβ monomers and membrane-bound Aβ were separated by ultracentrifugation at 200000*g* and 37 °C for 3 h. The peptide concentration in the supernatant was determined by analytical HPLC, which was performed using a COSMOSIL protein-R Packed Column (4.6 mm × 180 mm) (Nacalai Tesque, Kyoto, Japan) eluted with a linear gradient of $CH_3CN$ (20 to 60% over 40 min) in 0.1% aqueous trifluoroacetic acid at a flow rate of 1 mL/min. The protein was detected by measuring the UV absorbance at 220 nm.

**CD Spectra.** The concentration of Aβ in NaF buffer was 15 μM. CD spectra were recorded on a Jasco J-820 apparatus at 37 °C, using a 1 mm path length quartz cell to minimize the absorbance due to buffer components. The instrumental outputs were calibrated with nonhygroscopic ammonium *d*-camphor-10-sulfonete.[27] Eight scans were averaged for each sample. The blank spectra (SUV suspension or buffer) were subtracted.

**Thioflavin T (ThT) Assay.** The sample (final Aβ concentration of 0.5 μM) was added to a 5 μM ThT solution in 50 mM glycine buffer (pH 8.5). Fluorescence at 490 nm was measured at an excitation wavelength of 446 nm at 25 °C.[4,28] A calcein solution (1 μM) in 10 mM Tris/150 mM NaCl/1 mM EDTA (pH 7.4) buffer was used as a standard to calibrate small day-to-day variations in fluorescence intensity.

**SVD Analysis.** The CD data measured for a range of $x$ values were arranged into a $M \times N$ matrix, $\mathbf{A}$ ($M$ and $N$ are the numbers of wavelength data points and $x$ values, respectively), so that the element in the $j$th row and the $i$th column corresponded to the $[\theta]$ value at the $j$th wavelength and the $i$th $x$ value. The data matrix was expressed as a linear combination of orthogonal basis functions and their weighting factors:

$$\mathbf{A} = \mathbf{U}\cdot\mathbf{W}\cdot\mathbf{V}^{\mathrm{T}} \quad (1)$$

where $\mathbf{U}$, $\mathbf{W}$, and $\mathbf{V}$ are $M \times N$, $N \times N$, and $N \times N$ matrices, respectively. The $i$th column of $\mathbf{U}$, $u_i$, represents the orthogonal basis CD curve. $\mathbf{W}\cdot\mathbf{V}^{\mathrm{T}}$ represents $x$ value-dependent weights for the individual basis ($\mathbf{V}^{\mathrm{T}}$, the transposed matrix of $\mathbf{V}$). $\mathbf{W}$ is the diagonal matrix of singular values, which are usually arranged by magnitude in descending order. The number of mathematically independent components ($L$) is the rank order of $\mathbf{A}$ in an ideal case without noise, whereas in a real case with noise, it should be estimated on the basis of (1) singular values, (2) the autocorrelation $C(u_i)$ of the $i$th base, (3) the shape of the basis function, and (4) reduced $\chi^2$ values of SVD reconstruction.[29] The autocorrelation reflecting the signal-to-noise ratio was calculated according to

$$C(u_i) = \sum_{j=1}^{M-1} U_{j,i}U_{j+1,i} \quad (2)$$

where $U_{j,i}$ is the $j$th element of the $i$th column of matrix $\mathbf{U}$. Because each column vector is normalized to unity, the maximum value of the autocorrelation is 1. For basis functions with many elements (>100 rows) that are subjectively smooth, autocorrelation values may exceed 0.99, whereas for those with significant variations between rows (typical of "noise"), the autocorrelation values will be much smaller than 1; a value of less than 0.8 indicates a signal-to-noise ratio approaching 1.[30]

## RESULTS

**Binding of Aβ.** The binding of Aβ-(1−40) to GM1/cholesterol/SM (4:3:3) SUVs was directly assessed by a combination of ultracentrifugation and analytical HPLC. Fibrillization by Aβ was not observed during the procedure (vide infra). The amount of membrane-bound Aβ per GM1 in the outer leaflet of liposomes, $x$ (moles per mole), was plotted as a function of the concentration of free Aβ, $c_f$ in Figure 1. The binding equilibrium could be expressed by Langmuir's

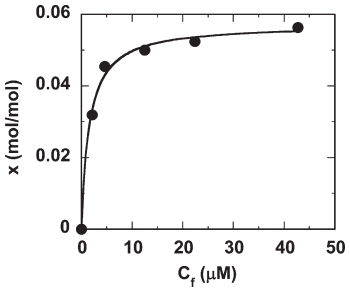


**Figure 1.** Binding isotherm of A$\beta$-(1−40) at 37 °C. The binding of the protein to GM1/cholesterol/SM (4:3:3) SUVs was directly assessed by ultracentrifugation and HPLC. The amount of membrane-bound A$\beta$ per GM1 in the outer leaflet, $x$, is plotted as a function of the concentration of free A$\beta$, $c_f$. The curve is a best fit by eq 3 with $x_{max}$ and $K$ values of 0.0573 and $6.53 \times 10^5$ $M^{-1}$, respectively.

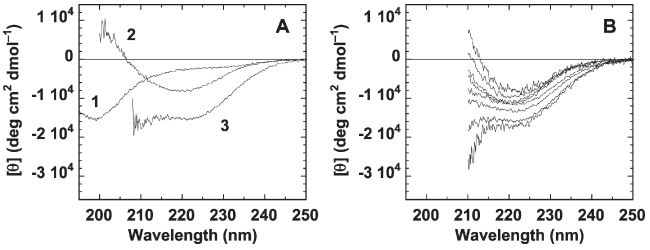


**Figure 2.** CD spectra of 15 $\mu$M A$\beta$-(1−40) at 37 °C. (A) Representative raw spectra in the absence (trace 1) or presence of SUVs (trace 2, GM1:A$\beta$ ratio of 30; trace 3, GM1:A$\beta$ ratio of 120). (B) CD spectra of membrane-bound A$\beta$. The GM1:A$\beta$ ratios (and corresponding $x$ values) are 10 (0.0504), 20 (0.0479), 30 (0.0440), 40 (0.0391), 60 (0.0297), 80 (0.0233), 120 (0.0160), and 150 (0.0132), from top to bottom, respectively.

equation.

$$x = \frac{x_{max} K c_f}{1 + K c_f} \tag{3}$$

The maximal $x$ value and the binding constant are denoted by $x_{max}$ and $K$ ($M^{-1}$), respectively. The estimated $x_{max}$ and $K$ values were 0.0573 ± 0.0014 and (6.53 ± 0.88) × $10^5$ $M^{-1}$, respectively.

**Secondary Structures.** The conformation of A$\beta$ in the presence and absence of SUVs was estimated from CD spectra at 37 °C. Representative spectra are shown in Figure 2A. The spectrum of A$\beta$ in buffer was characteristic of a random coil conformation (trace 1). In the presence of smaller amounts of SUVs, the spectra exhibited a minimum at around 218 nm, reminiscent of $\beta$-sheet structures (trace 2). In contrast, at higher GM1:A$\beta$ ratios, A$\beta$ formed α-helix-rich structures as judged from double minima at around 210 and 222 nm (trace 3). Structural changes upon membrane binding were completed within the dead time of the CD measurement (<3 min). These results were consistent with our previous findings using NaCl as a salt,[15,18] showing that the use of NaF does not influence A$\beta$−GM1 interaction.

The CD spectra of the membrane-bound A$\beta$ were obtained by subtracting the contributions from free A$\beta$ (Figure 2B). The fraction of unbound A$\beta$ ($f$) was calculated using the binding parameters obtained above. The mean residue ellipticity of

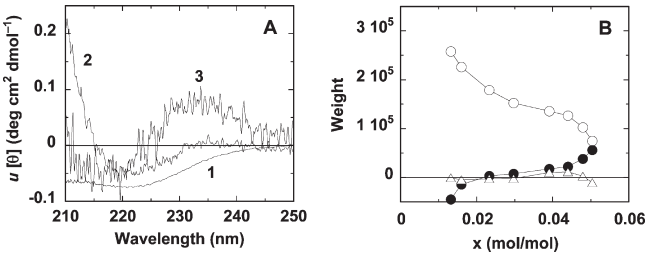


**Figure 3.** SVD analysis of CD spectra. CD spectra of membrane-bound A$\beta$ (Figure 2B) were analyzed by a SVD method. (A) Traces 1−3 denote the three basis spectra ($u_1$−$u_3$). See the text for details. (B) Weights for $u_1$ (○), $u_2$ (●), and $u_3$ (△) plotted as a function of $x$.

**Table 1. Results of SVD Analysis**

| ordinal number | singular value | autocorrelation |
|---|---|---|
| 1 | 472456 | 0.998 |
| 2 | 87684 | 0.970 |
| 3 | 19362 | 0.965 |
| 4 | 10136 | 0.688 |
| 5 | 6426 | 0.778 |
| 6 | 5147 | 0.710 |
| 7 | 3826 | 0.714 |
| 8 | 3147 | 0.725 |

bound A$\beta$ ($[\theta]_{bound}$) was calculated as follows:

$$[\theta]_{bound} = \frac{[\theta]_{obs} - f[\theta]_{free}}{1 - f} \tag{4}$$

The mean residue ellipticities of A$\beta$ determined in the presence and absence of liposomes are denoted by $[\theta]_{obs}$ and $[\theta]_{free}$, respectively.

The CD spectra of the membrane-bound A$\beta$ were analyzed by a SVD method[30] using IgorPro (WaveMetrics, Inc., Lake Oswego, OR) to extract the essential spectral components. The spectra below 210 nm were not used for the analysis because the signal-to-noise ratios of spectra at high GM1:A$\beta$ ratios were low. The sphingolipids with amide groups absorbed light in the far-UV region. Light scattering also led to deterioration of the quality of the spectra (the highest lipid concentration was 5.6 mM).

The results of the SVD analysis are summarized in Figure 3 and Table 1. The singular values and the autocorrelations (Table 1) clearly show that the first three components predominantly contribute to the original spectra ($L$ = 3). This conclusion is supported by spectral reconstitution (vide infra). The first basis spectrum, $u_1$, had a minimum around 222 nm, and the $[\theta]$ values were negative over the entire range of wavelengths, reminiscent of an α-helix. The second basis spectrum, $u_2$, exhibited a minimum around 220 nm, and the $[\theta]$ values changed from negative to positive above 215 nm, indicative of a $\beta$-sheet. In contrast, the third, far less intense spectrum, $u_3$, had two peaks of opposite sign and similar magnitude, characteristic of an exciton interaction between aromatic side chains.[31] The fourth to eighth spectra looked like noise (Figure S1 of the Supporting Information). Thus, there appear to be two main chain conformers (α-helix-rich and $\beta$-sheet-rich) aside from different side chain interactions.

The SVD analysis is, however, a pure mathematical procedure, and therefore, the basis spectra of columns of **U** do not

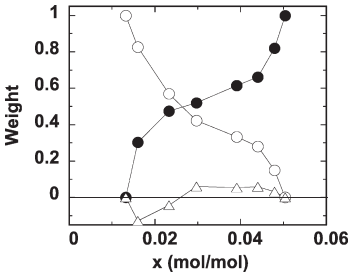


**Figure 4.** Transformation of basis spectra. The basis spectra $u_1-u_3$ were transformed into $u_1'-u_3'$, respectively, as described in the text. Weights $f_\alpha$, $f_\beta$, and $f_3$ for $u_1'$ (○), $u_2'$ (●), and $u_3'$ (△) are plotted as a function of $x$.

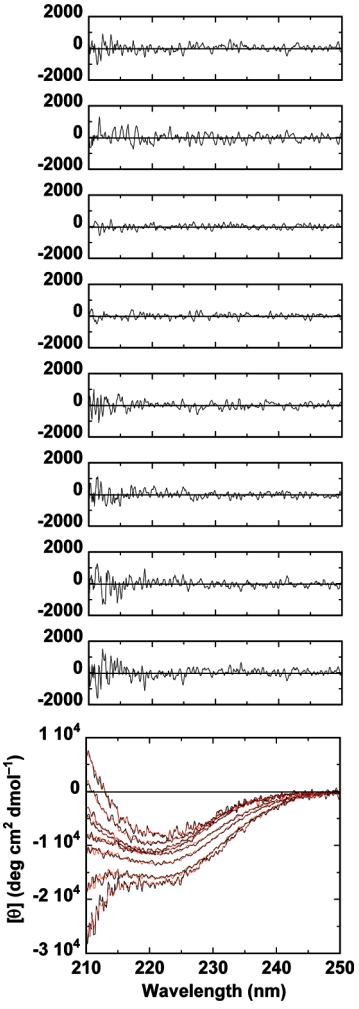


**Figure 5.** Reconstitution of CD spectra by linear combinations of $u_1'-u_3'$. The observed and reconstituted spectra are denoted by black and red traces, respectively, in the bottom panel. The residuals are shown in the top panels. The $x$ values are 0.0504, 0.0479, 0.0440, 0.0391, 0.0297, 0.0233, 0.0160, and 0.0132, from top to bottom, respectively. The nrmsd values for the fits were 0.0137, 0.0234, 0.0122, 0.0124, 0.0203, 0.0179, 0.0168, and 0.0114, respectively.

necessarily correspond to the actual spectra of the conformers. That is, $\mathbf{W}\cdot\mathbf{V}^{\mathrm{T}}$ does not give their fractions. Indeed, the weights for $u_2$ were negative at lower $x$ values (Figure 3B), indicating that the basis spectrum is imaginary. To estimate the fractions of the

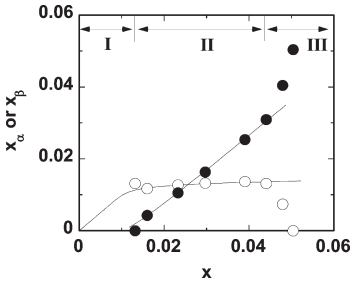


**Figure 6.** Concentrations of the α-helical and $\beta$-sheet species. The intramembrane concentrations of the α-helical ($x_\alpha$) and $\beta$-sheet ($x_\beta$) species were calculated with eqs 10 and 11, respectively, and are depicted with empty and filled circles, respectively. The lines indicate calculated values according to eq 12 with an $n$ of 15 and a $K$ of $5.8 \times 10^{24}$.

α-helix-rich and $\beta$-sheet-rich species, the orthogonal matrices **U**, **W**, and **V** were transformed into **U**′, **W**′, and **V**′, respectively, using the transformation matrix **R**, so that the column vectors of **U**′ give physically meaningful spectra.

$$\mathbf{U}' = \mathbf{U}\cdot\mathbf{R} \tag{5}$$

$$\mathbf{W}' = \mathbf{R}^{-1}\cdot\mathbf{W}\cdot\mathbf{R} \tag{6}$$

$$\mathbf{V}' = \mathbf{V}\cdot\mathbf{R} \tag{7}$$

$$\mathbf{V}'^{-1} = \mathbf{R}^{-1}\cdot\mathbf{V}^{-1} = \mathbf{R}^{-1}\cdot\mathbf{V}^{\mathrm{T}} \tag{8}$$

By using these transformed matrices, the original data matrix is expressed as

$$\mathbf{U}'\cdot\mathbf{W}'\cdot\mathbf{V}'^{-1} = \mathbf{U}\cdot\mathbf{R}\cdot\mathbf{R}^{-1}\cdot\mathbf{W}\cdot\mathbf{R}\cdot\mathbf{R}^{-1}\cdot\mathbf{V}^{-1} = \mathbf{U}\cdot\mathbf{W}\cdot\mathbf{V}^{\mathrm{T}} = \mathbf{A} \tag{9}$$

The transformation matrix, **R**, was determined as follows. The first and second column vectors of **U**′ were taken from the CD spectra at GM1:A$\beta$ ratios of 150 and 10. These spectra were taken to represent the α-helix-rich and $\beta$-sheet-rich species, respectively, because they did not change significantly with a further increase in the ratio to 180 or a decrease to 5 (Figure S2 of the Supporting Information). Next, the fraction of each secondary structure, $f_\alpha$ and $f_\beta$, was calculated for each spectrum at various GM1:A$\beta$ ratios from the values of the first and second rows of matrix $\mathbf{W}\cdot\mathbf{V}^{\mathrm{T}}$, respectively. $f_\alpha$, $f_\beta$, and the fraction of the third component ($f_3 = 1 - f_\alpha - f_\beta$) gave the first, second, and third rows of the transformed matrix $\mathbf{W}'\cdot\mathbf{V}'^{-1}$, respectively. Finally, the transformation matrix was obtained by $\mathbf{R}^{-1} = \mathbf{W}'\cdot\mathbf{V}'^{-1}\cdot\mathbf{V}\cdot\mathbf{W}^{-1}$. Figure 4 plots the fractional contribution ($f_\alpha$, $f_\beta$, and $f_3$) from each basis spectrum as a function of $x$. The $f_\alpha$ and $f_\beta$ values monotonously decreased and increased with an increase in $x$, respectively. In contrast, the $f_3$ value took both positive and negative values.

The observed spectra could be described well by linear combinations of $u_1'-u_3'$ (Figure 5). The average of the normalized root-mean-square deviation (nrmsd) values was 0.0160. Linear combinations of only $u_1'$ and $u_2'$ failed to reconstitute the spectra. The average nrmsd was 0.0287 (Figure S3 of the Supporting Information). The intramembrane concentrations of the α-helical ($x_\alpha$) and $\beta$-sheet ($x_\beta$) species were calculated with eqs 10 and 11, respectively, and are shown as a function of $x$

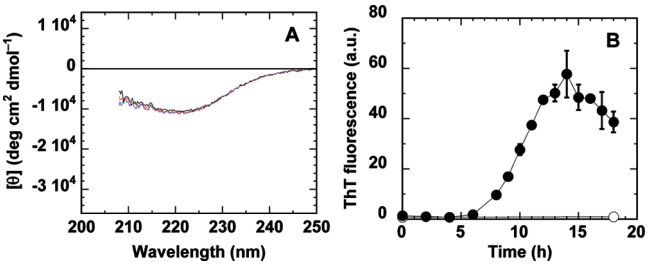


**Figure 7.** Stability of secondary structures of Aβ at 37 °C. (A) CD spectra of Aβ (15 μM) in the presence of SUVs (region II, $x = 0.0297$) recorded after incubation for 0 (black), 1 (red), and 8 days (blue). There were no detectable spectral changes. (B) In contrast, when $x = 0.0504$ (region III), an increase in ThT fluorescence is observed after a lag time of ~6 h (●). No ThT signal was observed in the absence of SUVs even after an 18 h incubation (○).

in Figure 6.

$$x_\alpha = \frac{f_\alpha}{f_\alpha + f_\beta} x \tag{10}$$

$$x_\beta = \frac{f_\beta}{f_\alpha + f_\beta} x \tag{11}$$

Interestingly, at $x$ values between 0.013 and 0.044 (region II), the $x_\alpha$ value was almost constant, whereas the $x_\beta$ value increased linearly above a threshold concentration of ~0.013. This unique behavior indicates that the α-helix-to-β-sheet transition occurs in a highly cooperative fashion like the formation of micelles of detergents or a phase separation and that a large number of molecules are involved in a β-sheet aggregate. If $n$ α-helix molecules form an $n$-meric β-sheet with association constant $K$, the equilibrium can be described by eq 12 (mole fraction ≈ $x$).

$$K = \frac{x_\beta / n}{{x_\alpha}^n} \tag{12}$$

The best fit was obtained with an $n$ of 15 and a $K$ of $5.8 \times 10^{24}$ ($\chi^2 = 0.00017$; $R = 0.88$) as shown by solid lines in Figure 6, although other combinations of $n$ and $K$ values ($n$ of 10 and $K$ of $1.2 \times 10^{16}$; $n$ of 20 and $K$ of $4.3 \times 10^{34}$) could also explain the results satisfactorily.

At $x$ values above 0.044 (region III), the amount of β-sheet species increased rapidly with the $x$ value at the expense of the α-helical conformer, suggesting the presence of an irreversible aggregation (vide infra).

**Kinetics and Mechanism of Aβ Aggregation.** The aggregation of Aβ in the presence of larger amounts of SUVs (region II, at $x = 0.0297$) was monitored using CD measurements (Figure 7A). The spectra did not show any change at least during an 8 day incubation at 37 °C, suggesting that the Aβ molecules on membranes were stable and did not enter the aggregation pathway, even though significant amounts of the β-sheet species were present. On the other hand, when $x = 0.0504$ (region III), the CD spectrum shows a flattening of signal intensity after incubation, indicating aggregation of Aβ (data not shown). The aggregation was monitored by an increase in the fluorescence intensity of the amyloid-specific dye ThT. While no increase in ThT fluorescence was detected without SUVs during an 18 h incubation, ThT fluorescence was increased after a 6 h lag phase and reached

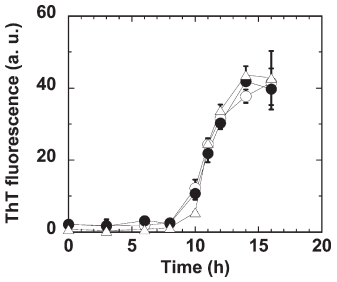


**Figure 8.** Aggregation kinetics of Aβ-(1−40) as monitored by the ThT assay. Aβ-(1−40) was incubated with GM1/cholesterol/SM (4:3:3) SUVs (30 μM GM1) at 37 °C. Aβ concentrations of (○) 30, (●) 45, and (△) 60 μM.

a maximum at 14 h in the presence of SUVs (Figure 7B). We have already confirmed the formation of amyloid fibrils by transmission electron microscopy.[25]

The elongation of amyloid fibrils is considered to proceed as follows.[1−6] A free monomer molecule in solution binds to a seed or a fibril end that acts as a template, changing its conformation. The bound molecule serves as a new fibril end to which another monomer binds. Repetition of this reaction results in the outgrowth of amyloid fibrils. In the formation of fibrils on membranes, both free monomers in solution (mechanism 1) and membrane-bound monomers (mechanism 2), in principle, can bind to seeds. We distinguished these two mechanisms as follows.

The concentration of the fibril-growing sites, which is the sum of the concentrations of seeds and fibril ends, is denoted by [GS]. The rate ($r_1$ or $r_2$) of fibril elongation in each mechanism can be expressed as follows.

$$r_1 = k_1[\text{free A}\beta\text{ monomer}][\text{GS}] \tag{13}$$

$$r_2 = k_2[\text{bound A}\beta\text{ monomer}][\text{GS}] \tag{14}$$

When the concentration of liposomes is sufficiently smaller than the concentration of Aβ in solution, almost all Aβ molecules exist as free monomers ([free Aβ] ~ [total Aβ]) and the binding site on the membrane is saturated ($x \sim x_{max}$). Therefore, the concentration of bound Aβ monomer is independent of the total concentration of Aβ when the liposome concentration is fixed. Although the rate of seed formation is dependent on $x$, [GS] is independent of [total Aβ] because $x \sim x_{max}$. As a consequence, $r_1$ is proportional to only [total Aβ] and $r_2$ is constant. If the elongation kinetics obey mechanism 1, the kinetics of ThT fluorescence increase, which were normalized by [total Aβ] (see Materials and Methods), should be independent of [total Aβ]. On the other hand, the rate of ThT fluorescence development is expected to be inversely slowed with an increase in [total Aβ] in mechanism 2. To achieve these conditions, we chose a concentration of SUVs of 30 μM (as GM1), i.e., 0.86 μM binding site, and Aβ concentrations of 30, 45, and 60 μM (see Figure 1). The results of ThT assays are shown in Figure 8. The fibrillization kinetics of the three samples were superimposable, indicating that the elongation of Aβ fibrils on GM1-containing membranes obeys mechanism 1, in which free Aβ in solution is recruited to growing fibrils.

## DISCUSSION

Helical forms have been suggested to be intermediates in the aggregation of Aβ[18,22,32−34] and other amyloidogenic

proteins[35−41] in solution,[32,33] detergent micelles,[22,34] and lipid bilayers.[18,35,36,39,40] Such structures are useful for the development of small molecules that inhibit the aggregation of Aβ.[42−44] However, the molecular details of the α-helix-to-β-sheet transitions are poorly understood. We clarified the structural transitions of Aβ-(1−40) mediated by GM1 clusters using CD spectroscopy and a SVD analysis.

To analyze the structural changes in the membrane phase, spectral contributions from free protein molecules were corrected by directly determining free concentrations. The binding isotherm (Figure 1) could be fitted by Langmuir's equation. However, this fit was phenomenological. This equation assumes that bound protein molecules do not interact with each other. This assumption clearly contradicts the cooperative formation of β-sheet aggregates. The association of peptides with lipid bilayers has been described by a partition equilibrium model combined with the Gouy−Chapman theory that takes electrostatic interaction between peptides and lipids into consideration.[45,46] In this case, a binding model is more appropriate, because GM1 clusters constitute binding sites for Aβ.[15,47] Electrostatic repulsion between negatively charged Aβ and GM1 gives negative cooperativity, which is apparently compensated by positive cooperativity in the α-helix-to-β-sheet transition.

CD spectra of membrane-bound Aβ were analyzed by the SVD method, which has been successfully used in protein folding studies.[29,48,49] The analysis indicated that Aβ assumes only two main chain conformers, i.e., an α-helix-rich structure and a β-sheet-rich structure in raftlike membranes containing GM1 clusters; however, the protein takes three states (Figure 6). In the diluted regime (region I, $x < \sim 0.013$), Aβ assumes only the α-helix-rich structure. A similar phenomenon was found for islet amyloid polypeptides in phospholipid bilayers.[36] The helicity was estimated to be ∼50% from a $[\theta]_{222}$ value of −17500 deg cm$^2$ dmol$^{-1}$.[50] Utsumi et al. reported that His$^{14}$−Val$^{24}$ and Ile$^{31}$−Val$^{36}$ segments (helicity of 53%) form α-helices in lyso-GM1 micelles at neutral pH, as determined by NMR spectroscopy.[51]

From a threshold concentration ($x$) from ≈0.013 to ≈0.044 (region II), an α-helix-to-β-sheet transition occurs in a highly cooperative fashion similar to the formation of a micelle, in which the concentration of the monomer is almost constant. The helical form coexists with β-sheet-rich aggregates composed of 10−20 protein molecules. The α-helix-to-β-sheet transition of Aβ dependent on the protein-to-lipid ratio was originally observed in phospholipid bilayers.[52] Recently, a temperature-dependent α-helix-to-β-sheet transition was also reported in dipalmitoylphosphatidylcholine bilayers.[53] According to the thermodynamics of micelle formation,[54] the difference in the standard Gibbs free energy between the aggregate and the monomer is approximated by eq 15.

$$\frac{G^0_{n\text{-mer}}}{n} - G^0_{\text{monomer}} \approx RT\, ln(\text{critical micellar concentration}) \quad (15)$$

where $R$ is the gas constant and $T$ is the absolute temperature. A critical concentration of 0.013 gives a standard free energy of $-4.3RT$ for the formation of an aggregate (−11 kJ/mol at 37 °C). Comparable values have been estimated for the formation of a β-sheet aggregate by penetratin, although our estimate includes energy necessary for the protein to deform the membrane. Assuming that 20 residues are involved in the formation of the β-sheet, the difference in free energy between the α-helix-rich form and the β-sheet-rich form is only −0.5 kJ/residue. The residual free energy of the membrane-induced formation of a β-structure has been reported to be close to that of the membrane-induced formation of an α-helix.[46]

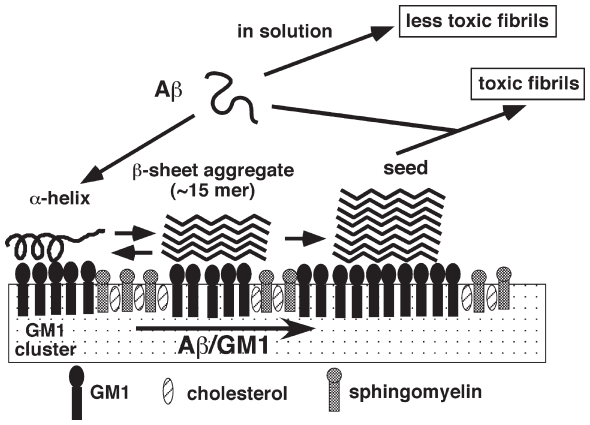


**Figure 9.** Schematic representation of the proposed interaction of Aβ with membranes containing GM1 clusters. Aβ specifically binds to a GM1 cluster, changing its conformation from a random coil to an α-helix-rich structure. At Aβ:GM1 ratios between ∼0.013 and ∼0.044, the helical species and aggregated β-sheets (∼15-mer) co-exist. However, the β-structure is stable and does not form larger aggregates. At Aβ:GM1 ratios above ∼0.044, the β-structure is converted to a second, seed-prone β-structure. The seed recruits monomers from the aqueous phase to form amyloid fibrils, the structure and toxicity of which are different from those of amyloids formed in solution.

The β-sheet aggregate does not form amyloids (Figure 7A). A seed-prone β-structure is generated after a second structural transition around $x \approx 0.044$ (region III, Figure 7B). The second β-sheet aggregate cannot be distinguished from the first in terms of secondary structure, suggesting that changes in mutual orientations of β-strands, including a shift in registry, are involved in this process. The changes in $f_3$ with respect to the $x$ value also support the existence of two transitions. The $f_3$ value first decreases, then increases, and finally decreases again. Phe residues may be involved in the exciton interaction. Roy et al. synthesized a β-hairpin peptide with a Phe−Phe interaction and observed a positive CD band at 221 nm and a negative band at 234 nm.[31] These wavelengths are close to ours (∼215 and ∼234 nm, respectively).

At $x$ values larger than ∼0.05, the seed-prone β-sheet is the predominant species in the membrane. A pioneering work by Terzi et al. clearly showed that Aβ-(1−40) is in a random coil−β-sheet equilibrium under these conditions in the presence of negatively charged phospholipid bilayers.[55]

On the basis of these results, we propose a revised scheme for the formation of amyloid fibrils by Aβ mediated by GM1 clusters (Figure 9). Aβ specifically binds to a GM1 cluster, changing its conformation from a random coil to an α-helix-rich structure with ∼50% helicity. At lower protein densities (Aβ:GM1 ratio of less than ∼0.013), only the helical species exists. At intermediate protein densities (Aβ:GM1 ratio between ∼0.013 and ∼0.044), the helical species and aggregated β-sheets (∼15-mer) coexist. However, the β-structure is stable and does not form larger aggregates. At Aβ/GM1 values above ∼0.044, the β-structure is converted to a second, seed-prone β-structure. The seed recruits monomers from the aqueous phase to form amyloid fibrils, the

structure and toxicity of which are different from those of amyloids formed in solution. These results will shed light on molecular mechanisms for the pathogenesis of the disease.

## ■ ASSOCIATED CONTENT

**Supporting Information.** CD basis spectra $u_4-u_8$, CD spectra of membrane-bound A$\beta$ at extreme GM1:$\beta$ ratios, and reconstituted CD spectra by linear combinations of only $u_1'$ and $u_2'$. This material is available free of charge via the Internet at http://pubs.acs.org.

## ■ AUTHOR INFORMATION

### Corresponding Author

*Phone: +81 75-753-4521. Fax: +81 75-753-4578. E-mail: katsumim@pharm.kyoto-u.ac.jp.

### Present Addresses

†Institute for Protein Research, Osaka University, 3-2 Yamadaoka, Suita, Osaka 565-0871, Japan.

### Funding Sources

This work was supported in part by The Research Funding for Longevity Sciences (22-14) from the National Center for Geriatrics and Gerontology (NCGG), Japan.

## ■ ABBREVIATIONS

A$\beta$, amyloid $\beta$-protein; AD, Alzheimer's disease; CD, circular dichroism; GM1, monosialoganglioside GM1; HPLC, high-performance liquid chromatography; nrmsd, normalized root-mean-square deviation; SM, *N*-acyl-D-sphingosine-1-phosphocholine from bovine brain; SUV, small unilamellar vesicle; SVD, singular-value decomposition; ThT, thioflavin T.

## ■ REFERENCES

(1) Jarrett, J. T., and Lansbury, P. T., Jr. (1993) Seeding "one-dimensional crystallization" of amyloid: A pathogenic mechanism in Alzheimer's disease and scrapie? *Cell 73*, 1055–1058.

(2) Naiki, H., Hasegawa, K., Yamaguchi, I., Nakamura, H., Gejyo, F., and Nakakuki, K. (1998) Apolipoprotein E and antioxidants have different mechanisms of inhibiting Alzheimer's $\beta$-amyloid fibril formation in vitro. *Biochemistry 37*, 17882–17889.

(3) Naiki, H., and Nakakuki, K. (1996) First-order kinetic model of Alzheimer's $\beta$-amyloid fibril extension in vitro. *Lab. Invest. 74*, 374–383.

(4) Naiki, H., and Gejyo, F. (1999) Kinetic analysis of amyloid fibril formation. *Methods Enzymol. 309*, 305–318.

(5) Oosawa, F., and Asakura, S. (1975) *Thermodynamics of the polymerizaiton of protein*, Academic Press, London.

(6) Murphy, R. M. (2007) Kinetics of amyloid formation and membrane interaction with amyloidogenic proteins. *Biochim. Biophys. Acta 1768*, 1923–1934.

(7) Gorbenko, G. P., and Kinnunen, P. K. (2006) The role of lipid−protein interactions in amyloid-type protein fibril formation. *Chem. Phys. Lipids 141*, 72–82.

(8) Sani, M. A., Gehman, J. D., and Separovic, F. (2011) Lipid matrix plays a role in A$\beta$ fibril kinetics and morphology. *FEBS Lett. 585*, 749–754.

(9) Selkoe, D. J. (1994) Cell biology of the amyloid $\beta$-protein precursor and the mechanism of Alzheimer's disease. *Annu. Rev. Cell Biol. 10*, 373–403.

(10) Hardy, J., and Selkoe, D. J. (2002) The amyloid hypothesis of Alzheimer's disease: Progress and problems on the road to therapeutics. *Science 297*, 353–356.

(11) Seubert, P., Vigo-Pelfrey, C., Esch, F., Lee, M., Dovey, H., Davis, D., Sinha, S., Schlossmacher, M., Whaley, J., Swindlehurst, C., McCormack, R., Wolfert, R., Selkoe, J., Lieberburg, I., and Schenk, D. (1992) Isolation and quantification of soluble Alzheimer's $\beta$-peptide from biological fluids. *Nature 359*, 325–327.

(12) O'Nuallain, B., Shivaprasad, S., Kheterpal, I., and Wetzel, R. (2005) Thermodynamics of A$\beta$(1−40) amyloid fibril elongation. *Biochemistry 44*, 10709–12718.

(13) Matsuzaki, K. (2007) Physicochemical interactions of amyloid $\beta$-peptide with lipid bilayers. *Biochim. Biophys. Acta 1768*, 1935–1942.

(14) Matsuzaki, K., Kato, K., and Yanagisawa, K. (2010) A$\beta$ polymerization through interaction with membrane gangliosides. *Biochim. Biophys. Acta 1801*, 868–877.

(15) Kakio, A., Nishimoto, S., Yanagisawa, K., Kozutsumi, Y., and Matsuzaki, K. (2001) Cholesterol-dependent formation of GM1 ganglioside-bound amyloid $\beta$-protein, an endogenous seed for Alzheimer amyloid. *J. Biol. Chem. 276*, 24985–24990.

(16) Yanagisawa, K. (2007) Role of gangliosides in Alzheimer's disease. *Biochim. Biophys. Acta 1768*, 1943–1951.

(17) Ariga, T., McDonald, M. P., and Yu, R. K. (2008) Role of ganglioside metabolism in the pathogenesis of Alzheimer's disease: A review. *J. Lipid Res. 49*, 1157–1175.

(18) Kakio, A., Nishimoto, S., Yanagisawa, K., Kozutsumi, Y., and Matsuzaki, K. (2002) Interactions of amyloid $\beta$-protein with various gangliosides in raft-like membranes: Importance of GM1 ganglioside-bound form as an endogenous seed for Alzheimer amyloid. *Biochemistry 41*, 7385–7390.

(19) Lee, E. K., Hwang, J. H., Shin, D. Y., Kim, D. I., and Yoo, Y. J. (2005) Production of recombinant amyloid-$\beta$ a peptide 42 as an ubiquitin extension. *Protein Expression Purif. 40*, 183–189.

(20) Yamaguchi, T., Yagi, H., Goto, Y., Matsuzaki, K., and Hoshino, M. (2010) A disulfide-linked amyloid-$\beta$ peptide dimer forms a protofibril-like oligomer through a distinct pathway from amyloid fibril formation. *Biochemistry 49*, 7100–7107.

(21) Yang, J. T., Wu, C.-S. C., and Martinez, H. M. (1986) Calculation of protein conformation from circular dichroism. *Methods Enzymol. 130*, 208–269.

(22) Okada, T., Wakabayashi, M., Ikeda, K., and Matsuzaki, K. (2007) Formation of toxic fibrils of Alzheimer's amyloid $\beta$-protein-(1−40) by monosialoganglioside GM1, a neuronal membrane component. *J. Mol. Biol. 371*, 481–489.

(23) Svennerholm, L. (1957) Quantitative estimation of sialic acids. II. A colorimetric resorcinol-hydrochloric acid method. *Biochim. Biophys. Acta 24*, 604–611.

(24) Bartlett, G. R. (1959) Phosphorus assay in column chromatography. *J. Biol. Chem. 234*, 466–468.

(25) Matsuzaki, K., Noguch, T., Wakabayashi, M., Ikeda, K., Okada, T., Ohashi, Y., Hoshino, M., and Naiki, H. (2007) Inhibitors of amyloid $\beta$-protein aggregation mediated by GM1-containing raft-like membranes. *Biochim. Biophys. Acta 1768*, 122–130.

(26) Yamamoto, N., Matsuzaki, K., and Yanagisawa, K. (2005) Cross-seeding of wild-type and hereditary variant type amyloid $\beta$-proteins in the presence of gangliosides. *J. Neurochem. 95*, 1167–1176.

(27) Takakuwa, T., Konno, T., and Meguro, H. (1985) A new standard substance for calibration of circular dichroism: Ammonium *d*-10-camphorsulfonate. *Anal. Sci. 1*, 215–218.

(28) LeVine, H., III (1993) Thioflavine T interaction with synthetic Alzheimer's disease $\beta$-amyloid peptides: Detection of amyloid aggregation in solution. *Protein Sci. 2*, 404–410.

(29) Kojima, M., Tanokura, M., Maeda, M., Kimura, K., Amemiya, Y., Kihara, H., and Takahashi, K. (2000) pH-dependent unfolding of aspergillopepsin II studied by small-angle X-ray scattering. *Biochemistry 39*, 1364–1372.

(30) Henry, E. R., and Hofrichter, J. (1992) Singular value decomposition: Application to analysis of experimental data. *Methods Enzymol. 210*, 129–192.

(31) Roy, R. S., Gopi, H. N., Raghothama, S., Gilardi, R. D., Karle, I. L., and Balaram, P. (2005) Peptide hairpins with strand segments

containing α- and β-amino acid residues: Cross-strand aromatic interactions of facing Phe residues. *Biopolymers 80*, 787–799.

(32) Kirkitadze, M. D., Condron, M. M., and Teplow, D. B. (2001) Identification and characterization of key kinetic intermediates in amyloid β-protein fibrillogenesis. *J. Mol. Biol. 312*, 1103–1119.

(33) Fezoui, Y., and Teplow, D. B. (2002) Kinetic studies of amyloid β-protein fibril assembly. Differential effects of α-helix stabilization. *J. Biol. Chem. 277*, 36948–36954.

(34) Mandal, P. K., and Pettegrew, J. W. (2004) Alzheimer's disease: Soluble oligomeric Aβ(1−40) peptide in membrane mimic environment from solution NMR and circular dichroism studies. *Neurochem. Res. 29*, 2267–2272.

(35) Jayasinghe, S. A., and Langen, R. (2005) Lipid membranes modulate the structure of islet amyloid polypeptide. *Biochemistry 44*, 12113–12119.

(36) Knight, J. D., Hebda, J. A., and Miranker, A. D. (2006) Conserved and cooperative assembly of membrane-bound α-helical states of islet amyloid polypeptide. *Biochemistry 45*, 9496–9508.

(37) Olofsson, A., Borowik, T., Gröbner, G., and Sauer-Eriksson, A. E. (2007) Negatively charged phospholipid membranes induce amyloid formation of medin via an α-helical intermediate. *J. Mol. Biol. 374*, 186–194.

(38) Abedini, A., and Raleigh, D. P. (2009) A critical assessment of the role of helical intermediates in amyloid formation by natively unfolded proteins and polypeptides. *Protein Eng., Des. Sel. 22*, 453–459.

(39) Lee, C.-C., Sun, Y., and Huang, H. W. (2010) Membrane-mediated peptide conformation change from α-monomers to β-aggregates. *Biophys. J. 98*, 2236–2245.

(40) Sun, Y., Lee, C.-C., Chen, T.-H., and Huang, H. W. (2010) Kinetic process of β-amyloid formation via membrane binding. *Biophys. J. 99*, 544–552.

(41) Butterfield, S. M., and Lashuel, H. A. (2010) Amyloidogenic protein-membrane interactions: Mechanistic insight from model systems. *Angew. Chem., Int. Ed. 49*, 5628–5654.

(42) Choi, J.-S., Braymer, J. J., Nanga, R. P. R., Ramamoorthy, A., and Lim, M. H. (2010) Design of small molecules that target metal-Aβ species and regulate metal-induced Aβ aggregation and neurotoxicity. *Proc. Natl. Acad. Sci. U.S.A. 107*, 21990–21995.

(43) Hindo, S. S., Mancino, A. M., Braymer, J. J., Liu, Y., Vivekanandan, S., Ramamoorthy, A., and Lim, M. H. (2009) Small molecule modulators of copper-induced Aβ aggregation. *J. Am. Chem. Soc. 131*, 16663–16665.

(44) Yoo, S. I., Yang, M., Brender, J. R., Subramanian, V., Sun, K., Joo, N. E., Jeong, S. H., Ramamoorthy, A., and Kotov, N. A. (2011) Inhibition of amyloid peptide fibrillation by inorganic nanoparticles: Functional similarities with proteins. *Angew. Chem., Int. Ed. 50*, 5110–5115.

(45) Wieprecht, T., Beyermann, M., and Seelig, J. (1999) Binding of antibacterial magainin peptides to electrically neutral membranes: Thermodynamics and structure. *Biochemistry 38*, 10377–10387.

(46) Meier, M., and Seelig, J. (2007) Thermodynamics of the coil−β-sheet transition in a membrane environment. *J. Mol. Biol. 369*, 277–289.

(47) Mikhalyov, I., Olofsson, A., Gröbner, G., and Johansson, L. B. (2010) Designed fluorescent probes reveal interactions between amyloid-β(1−40) peptides and GM1 gangliosides in micelles and lipid vesicles. *Biophys. J. 99*, 1510–1519.

(48) Konno, T. (1998) Conformational diversity of acid-denatured cytochrome c studied by a matrix analysis of far-UV CD spectra. *Protein Sci. 7*, 975–982.

(49) Kamiyoshihara, T., Kojima, M., Uéda, K., Tashiro, M., and Shimotakahara, S. (2007) Observation of multiple intermediates in α-synuclein fibril formation by singular value decomposition analysis. *Biochem. Biophys. Res. Commun. 355*, 398–403.

(50) Chen, Y.-H., Yang, J. T., and Martinez, H. M. (1972) Determination of the secondary structures of proteins by circular dichroism and optical rotatory dispersion. *Biochemistry 11*, 4120–4131.

(51) Utsumi, M., Yamaguchi, Y., Sasakawa, H., Yamamoto, N., Yanagisawa, K., and Kato, K. (2008) Up-and-down topological mode of amyloid β-peptide lying on hydrophilic/hydrophobic interface of ganglioside clusters. *Glycoconjugate J. 26*, 999–1006.

(52) Terzi, E., Hölzemann, G., and Seelig, J. (1997) Interaction of Alzheimer β-amyloid peptide(1−40) with lipid membranes. *Biochemistry 36*, 14845–14852.

(53) Yoda, M., Miura, T., and Takeuchi, H. (2008) Non-electrostatic binding and self-association of amyloid β-peptide on the surface of tightly packed phosphatidylcholine membranes. *Biochem. Biophys. Res. Commun. 376*, 56–59.

(54) Daune, M. (1999) Hydrophobic and hydrophilic molecules. In *Molecular biophysics*, Chapter 12, Oxford University Press, New York.

(55) Terzi, E., Hölzmann, G., and Seelig, J. (1995) Self-association of β-amyloid peptide (1−40) in solution and binding to lipid membranes. *J. Mol. Biol. 252*, 633–642.